

METHODOLOGY

GRIM-filter: fast seed filtering in read mapping using emerging memory technologies

Jeremie S. Kim^{1*}, Damla Senol¹, Hongyi Xin², Donghyuk Lee³, Saugata Ghose¹, Mohammed Alser⁴, Hasan Hassan⁶, Oguz Ergin⁵, Can Alkan^{*4}, and Onur Mutlu^{*6,1}

*Correspondence:

jeremiekim123@gmail.com,
calkan@cs.bilkent.edu.tr,
onur.mutlu@inf.ethz.ch

¹Department of Electrical and
Computer Engineering, Carnegie
Mellon University, Forbes Avenue,
Pittsburgh, USA

Full list of author information is
available at the end of the article

Abstract

Motivation: Seed filtering is critical in DNA read mapping, a process where billions of DNA fragments (reads) sampled from a donor are mapped onto a reference genome to identify genomic variants of the donor. Read mappers 1) quickly generate possible mapping locations (i.e., seeds) for each read, 2) extract reference sequences at each of the mapping locations, and then 3) check similarity between each read and its associated reference sequences with a computationally expensive dynamic programming algorithm (alignment) to determine the origin of the read. Location filters come into play before alignment, discarding seed locations that alignment would have deemed a poor match. The ideal location filter would discard all poor matching locations prior to alignment such that there is no wasted computation on poor alignments.

Results: We propose a novel filtering algorithm, GRIM-Filter, optimized to exploit emerging 3D-stacked memory systems that integrate computation within a stacked logic layer, enabling processing-in-memory (PIM). GRIM-Filter quickly filters locations by 1) introducing a new representation of coarse-grained segments of the reference genome and 2) using massively-parallel in-memory operations to identify read presence within each coarse-grained segment. Our evaluations show that for 5% error acceptance rates, GRIM-Filter eliminates 5.59x-6.41x more false negatives and exhibits end-to-end speedups of 1.81x-3.65x compared to mappers employing the best previous filtering algorithm.

1 Introduction

Our understanding of human genomes today is affected by modern technology's ability to quickly and accurately determine an individual's entire genome. The human genome is comprised of a sequence of approximately 3 billion bases that are grouped into deoxyribonucleic acids (*DNA*), but today's machines can only identify DNA in short sequences (*reads*). Therefore, determining a genome requires 3 stages: 1) cutting the genome into many short fragments, 2) identifying the DNA sequence of the fragment, and then 3) mapping the reads against the reference genome in order to analyze the variations in the sequenced genome. In this paper, we focus on improving stage 3, often referred to as *read mapping*. Read mapping is performed computationally by *read mappers* after each read has been resolved into a known series of DNA.

We refer to Figure 1 to briefly explain a class of read mappers, seed-and-extend mappers. Seed-and-extend mappers attempt to find locations in the reference genome that closely match each read sequence with the following procedure. It 1) obtains a query read, 2) selects smaller segments (i.e., seeds) of the read, 3) index a data structure with these seeds to obtain a list of possible locations that would result in a match, 4) obtain the sequence from the reference genome, and 5) align the read sequence to the reference sequence with an expensive dynamic programming algorithm in order to determine similarity.

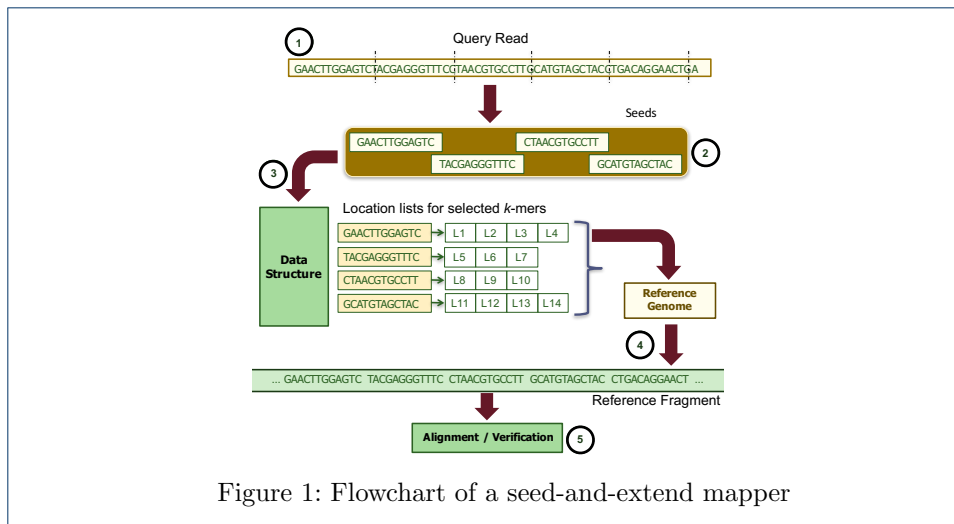


Figure 1: Flowchart of a seed-and-extend mapper

To improve performance on the runtimes of seed-and-extend mappers, we can utilize *seed filters*, recently introduced by Xin et al. [1]. Seed filters efficiently determine whether a candidate mapping location will result in an incorrect mapping *before* performing the computationally-expensive alignment step for that location. As long as the filter can eliminate possible locations faster than the time it takes to execute alignment, the entire read mapping process will be accelerated [1, 2]. As a result, several recent works have focused on optimizing the performance of seed filters [1–6].

The onset of seed filters has resulted in a shift of the performance bottleneck to filtering but filters still require large amounts of memory bandwidth to process and characterize each of the candidate locations. We attempt to reduce the time spent in filtering and present a new algorithm, GRIM-Filter, to efficiently filter locations with high parallelism. We observe that the characteristics of GRIM-Filter reflect an algorithm well-suited for implementation on 3D-stacked memory and evaluate GRIM-Filter on our in-house 3D-stacked memory simulator.

3D-stacked DRAM [7–12] is an available and emerging technology that integrates logic and memory in a 3D stack of dies with a large internal bandwidth. This enables the bulk transfer of data from memory to a logic layer that can perform simple parallel operations on the data.

Whereas conventional computing requires the movement of data on buses between core and memory, processing-in-memory (PIM)-enabled devices such as 3D-stacked memory enable simple arithmetic operations in nearby memory with high bandwidth. With carefully designed algorithms mapped for PIM, applications can often be improved immensely as the relatively small bus between core and memory no longer impedes the progress of computation on the data.

Our goal is to develop a seed filter that exploits the high memory bandwidth and processing-in-memory capabilities of 3D-stacked DRAM to increase the performance of hash table based read mappers without sacrificing their high sensitivity or comprehensiveness.

To our knowledge, this is the **first** seed filtering algorithm that accelerates read mapping by overcoming the memory bottleneck with PIM using 3D-stacked memory technologies. GRIM-Filter can be used with any read mapper, however, in this work we demonstrate the effectiveness of GRIM-Filter with a hash-table based mapper.

Key Mechanism. GRIM-Filter provides a quick method for determining whether a read will **not** match at a given location, thus allowing the read mapper to skip the expensive alignment process for that location. GRIM-Filter works by counting the existence of small segments of a read in a genome region. If the count falls under a threshold, GRIM-Filter discards the locations in that region before alignment. The existence of all small segments in a region are stored in a bit vector which can be easily predetermined for each region of a reference genome and retrieved when a read results in a potential location to a given region. We find that this regional approximation technique not only enables a high performance boost via parallelism but also improves filtering accuracy over the state-of-the-art.

Key Results. We evaluate GRIM-Filter qualitatively and quantitatively against the state-of-the-art seed filter *FastHASH* [1]. Our results show that GRIM-Filter yields a $5.59x$ – $6.41x$ smaller false negative rate (i.e., proportion of locations that pass the filter, but result in a poor match) than the best previous filter, and runs end-to-end $1.81x$ – $3.65x$ faster than *mrFAST* with *FastHASH* for a set of real genomic reads, when we use a 5% error threshold. We also note that as we increase the error rate, the performance of our filter over the state-of-the-art also increases, thus making our filter more effective and relevant for future generation error-prone sequencing technologies.

2 Motivation and Aim

Mapping the reads against the reference genome enables the analysis of the variations in the sequenced genome, and with a higher throughput in mapping sequences, more large-scale analyses are possible. The ability to deeply characterize and analyze genomes on a large scale could change medicine from reactive to a preventative and further personalized practice. In order to motivate our method of improving the performance of read mappers, we pinpoint the performance bottlenecks of modern-day mappers on which to focus our acceleration efforts. We find that across our dataset, *mrFAST* with *FastHASH* [1] still spends 15% of computation time aligning locations that are found to be a match, and 59% of the time aligning locations that are later discarded (i.e., *false locations*). Our goal is to implement a filter that reduces the wasted computation time spent aligning false locations by quickly determining if a location will not match the read and forgo the alignment altogether. The ideal filter would exhibit no additional overhead and correctly find all false locations and shows the potential to improve average performance of *mrFAST* on the same machine by $3.2x$. We note that this speedup is primarily earned by reducing the number of false location alignments, whereas most prior works gain their speedup by implementing parts or all of the read mapper in hardware. These works are orthogonal solutions, and could be implemented together with location filters for additional performance improvement.

3 GRIM-Filter

We now describe our proposal for a new seed filter, GRIM-Filter. At a high level, GRIM-Filter utilizes meta-data on short segments of the genome in order to quickly determine if a read will **not** result in a match at that genome segment.

Figure 2 shows a reference genome with its associated meta-data. The reference genome is divided into short contiguous segments, on the order of several hundreds of base pairs, which we refer to as *bins*. GRIM-Filter runs at the granularity of these bins, operating on the meta-data associated with each bin. This meta-data is stored in a *bit vector* that stores whether or not a *token*, or small DNA sequence on the order of 5 base pairs, can be found within the associated bin. We refer to each bit

as an *existence bit*. To account for all possible tokens of length n , each bit vector must be 2^n bits in length, where each bit denotes the existence of a particular token instance. Figure 2 highlights the bits of two token instances of bin_2 's bit vector showing the existence of token GACAG (green) with a 1 and the lack of token TTTTT (red) with a 0.

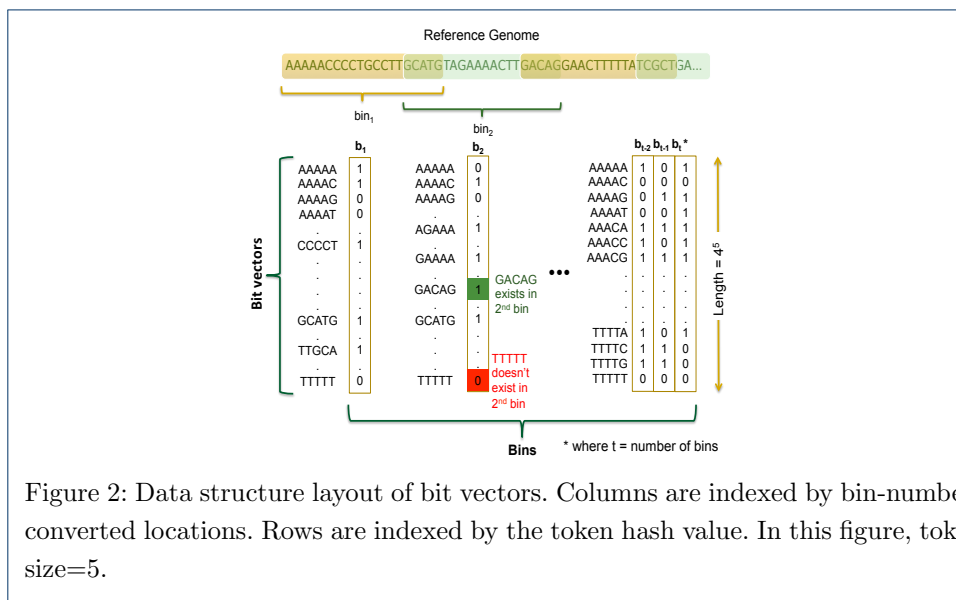


Figure 2: Data structure layout of bit vectors. Columns are indexed by bin-number-converted locations. Rows are indexed by the token hash value. In this figure, token size=5.

Because these bit vectors are associated with the reference genome, the bit vectors must only be generated once per reference and can be reused to map any number of reads from other individuals of the same species. However, in order to generate the bit vectors, the genome must be sequentially scanned for every sequence of n length tokens. If bin_x contains the first base pair of a token, the token's corresponding index of the associated $bitvector_x$ must be set (1), but otherwise unset (0). These bit vectors can then be saved for later reuse when mapping reads to the same reference genome used to generate them.

Before alignment, GRIM-Filter checks a read's potential mapping location by operating on the bit vector of the bin holding the first base pair of that read. This relies on the entire read being contained within a given bin, requiring bins to overlap (i.e., some base pairs are contained in multiple bins) as shown in Figure 2.

GRIM-Filter uses these bit vectors in order to quickly determine if a match within a given error rate is impossible. This is determined before running alignment, the expensive dynamic programming algorithm in order to reduce the number of unnecessary alignment operations. For each location, we 1) load the bit vector of the bin containing the location, 2) operate on the bit vector (as we will describe shortly) to quickly determine if there will be no match, and 3) discard the location if GRIM-Filter determines a poor match. Otherwise, the sequence at that location must be aligned with the read to determine the match similarity.

Using the circled steps in Figure 3, we explain in detail how GRIM-Filter determines whether to discard a location z for a read. 1) GRIM-Filter extracts every token in the read and 2) accumulates their respective existence bits from the bit vector. 3) The sums are compared to a threshold (that we explain below), and set to 1 if it meets the threshold, otherwise set to 0. When the read mapper is ready to align a read to a segment of the reference sequence, the read mapper must

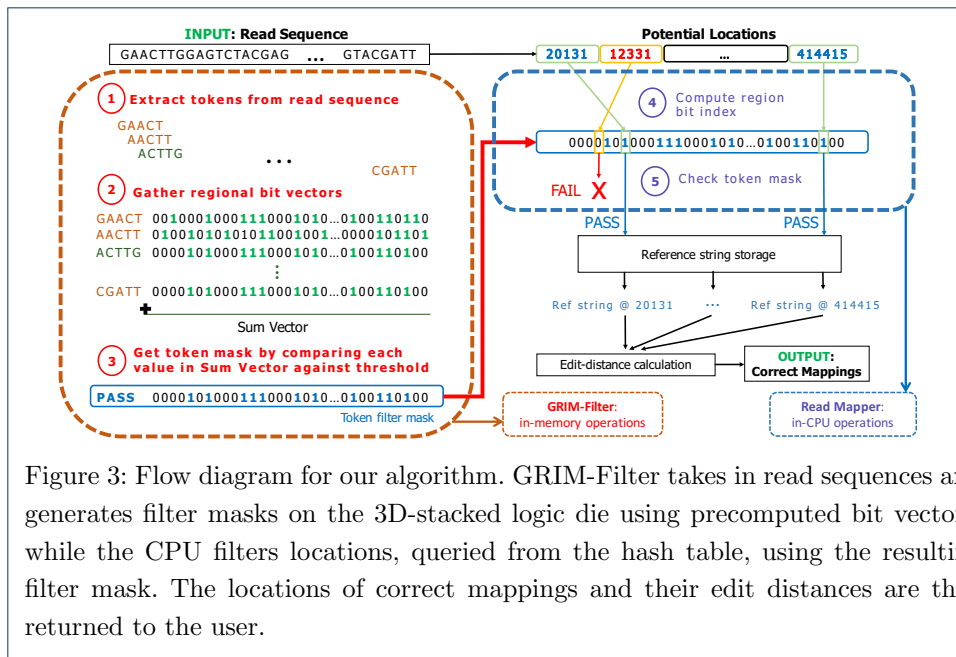


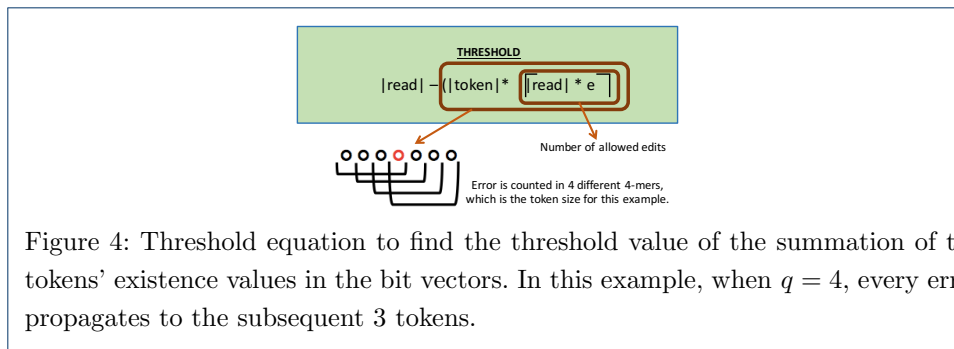
Figure 3: Flow diagram for our algorithm. GRIM-Filter takes in read sequences and generates filter masks on the 3D-stacked logic die using precomputed bit vectors, while the CPU filters locations, queried from the hash table, using the resulting filter mask. The locations of correct mappings and their edit distances are then returned to the user.

4) determine which bit to check against, and then 5) determine whether it should continue with alignment or not.

We now discuss in detail how to determine the threshold value to compare the sum from step 3. A higher sum would represent a higher probability for the read to match well within that bin, since a higher sum represents a higher number of parts of the read being found in the bin. However, intuitively, this may never confirm whether the read would match well or how well the match would be. On the other hand, if the number of parts found falls below a certain threshold, we can guarantee that the read will result in a poor match.

If reads mapped perfectly to the reference sequence, the threshold would simply be the total number of tokens in a read or $read.length - (n - 1)$. However, due to the need for allowing some differences in an alignment, we must compare the accumulation sum against a lower value taking into account the worst case error rate. This threshold can be calculated using the equation given in Figure 4. As shown in the figure, a token of size n in a bin overlaps with n other tokens. Assuming a single substitution error between the read and reference sequence, the error will propagate to the n previous tokens, meaning that those tokens may not be found in that bin. We determine that the equation in Figure 4 reflects the worst case error distribution and error rate (e.g., an error rate of 5% or less of the read length is widely used [2, 13–15]) in a good match. In the worst case, where the maximum number of errors occurs and every error affects the n adjacent tokens, the valid accumulation threshold is at its lowest value.

After comparing the accumulated sum against the threshold calculated using the appropriate values (read size, error rate threshold, and token size), GRIM-Filter returns control to the read mapper to align those locations that pass the filter. This process is repeated for all locations, which significantly reduces the number of alignment operations and ultimately reducing the end-to-end read mapping runtime.



3.1 Candidacy for 3D-stacked Memory Implementations

We identify **three** characteristics of GRIM-Filter that make it a great candidate implementing in for 3D-stacked memory: 1) only requires very simple operations, 2) highly parallelizable since each bin can be operated on independently, and 3) it is highly memory-bound requiring a single memory access for approximately every three instructions.

4 Mapping to 3D-Stacked Memory

In this section, we first introduce *3D-stacked DRAM* and describe how GRIM-Filter can be easily mapped to utilize this emerging technology, which attempts to bridge the disparity between processor speed and memory bandwidth. As this disparity increases, memory becomes more of a bottleneck in the computing stack [16]. Along with 3D-stacked DRAM, which enables much higher bandwidth and lower latency compared to conventional DRAM, the disparity between processor and memory is alleviated by the re-emergence of *Processing-in-Memory*, which integrates processing units inside or near the memory system to leverage high in-DRAM bandwidth and reduce energy consumption by reducing the amount of data transferred to the processor. In this section, we briefly explain the required background for these two technologies, which we will leverage to accelerate DNA read mapping.

4.1 3D-Stacked Memory

3D-stacked DRAM has a much higher internal bandwidth than conventional DRAM, thanks to the closer integration of logic and memory using *through-silicon via* (TSV) technology as seen in Figure 5. TSVs are vertical interconnects that can pass through the silicon wafers of a 3D stack of dies [17]. TSVs have a much smaller feature size than a standard interconnect, which enables a 3D-stacked DRAM to integrate hundreds to thousands of these wired connections between stacked layers. Using these wide wired connections, 3D-stacked DRAM can transfer bulk data simultaneously, enabling much higher bandwidth compared to conventional DRAM. Figure 5 shows a 3D-stacked DRAM (High Bandwidth Memory, HBM [7]) based system that consists of a 4-layer stacked DRAM using TSVs, a processor die, and silicon interposer that connects the stacked DRAM and the processor. The vertical connections in the stacked DRAM are very wide and very short which results in *high bandwidth* and *low power consumption*, respectively [8]. There exist many different 3D-stacked DRAM architectures available today. High Bandwidth Memory (HBM) is already integrated into the new AMD RadeonTM R9 Series Graphics Cards [9] and NVIDIA also announced that they will use HBM in their future products [10]. Hybrid Memory Cube (HMC) is also being developed by a number of different contributing companies [11, 12]. Other new technologies are also around the corner and

can enable processing-in-memory, such as Micron’s Automata Processor (AP) [18] and Tibco transactional application servers [19, 20].

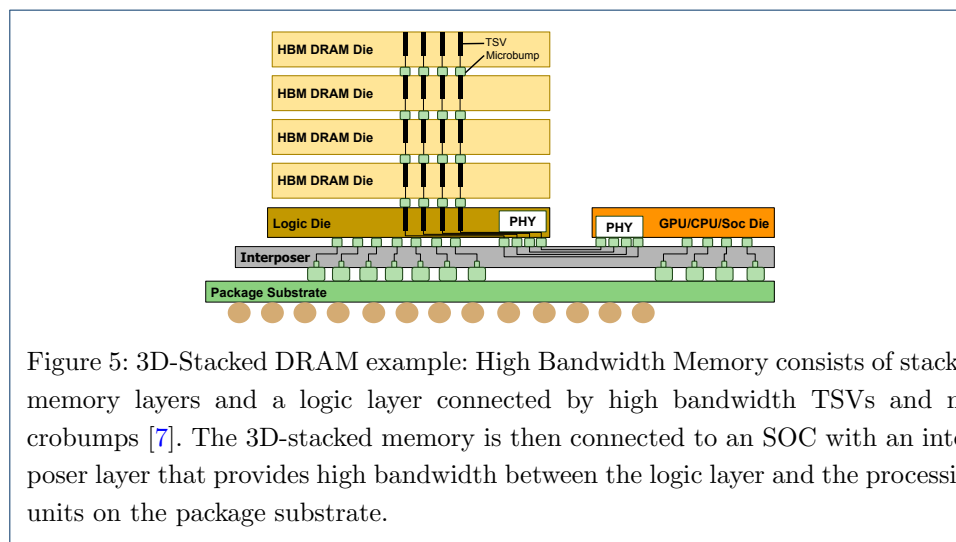


Figure 5: 3D-Stacked DRAM example: High Bandwidth Memory consists of stacked memory layers and a logic layer connected by high bandwidth TSVs and microbumps [7]. The 3D-stacked memory is then connected to an SOC with an interposer layer that provides high bandwidth between the logic layer and the processing units on the package substrate.

Processing-in-Memory. A key technique to increase the memory system bandwidth and reduce energy consumption in the memory system is placing computation units inside the memory system (e.g., PIM). Today, we see processing capabilities appearing in or near conventional DRAM [8, 21–25]. By enabling computation within or near the memory system and only transferring the results to the CPU, PIM provides significant performance improvements and energy reductions compared to the conventional system architecture that transfers all data to the process and only executes instructions within the CPU [21, 22, 26, 27].

3D-stacked DRAM with PIM. Combining these two new technologies, 3D-stacked DRAM and PIM enable great opportunities to build very high performance systems. A popular architecture for proposed 3D-stacked DRAM consists of multiple stacked memory layers and a logic layer that control the stacked memory, as shown in Figure 5. As many prior works show [21, 22, 26–29], the logic layer in 3D-stacked DRAM can be utilized not only for managing the stacked memory layers, but also for integrating application-specific accelerators. Since the logic layer already exists and has enough space to integrate compute units, integrating application-specific accelerators in the logic layer requires very small design and implementation overhead and little to no hardware overhead. 3D-stacked DRAM architecture enables us to fully customize the logic layer for the acceleration of applications [22, 29].

4.2 Mapping GRIM-Filter

We use mrFAST with FastHASH [1] as our baseline for code and performance. Our bit vector based implementation exists as an extension to FastHASH as a simple series of calls to an Application Programming Interface (API). FastHASH has an inflexible set of parameters, so there is not as much system-specific tuning that can be done. However, for shared data structures between FastHASH and GRIM-Filter, all parameters are kept consistent for a fair comparison. For those parameters specific to the bit vectors data structure in GRIM, we run tests to find a set of parameters that result in a highly effective filter for our system (shown in Section 6).

Due to the simplicity of our bit vector algorithm, we claim a low development and area cost for the logic layer in the 3D-stacked memory device. The required hardware for the logic layer as seen in Figure 6 simply depends upon the bandwidth available directly from the memory layers via TSVs.

GRIM-Filter involves reading p bits (*existence bits*) in parallel from differing bins representing the bin existence for the same token. We distribute our bit vectors throughout memory such that 1) every bit representing the existence of a given token across all bins is allocated a contiguous region of memory, and 2) all bits describing a given bin n from bit vectors of different tokens will fall in the same column. We then use these existence bits to increment the accumulator in the corresponding indices and repeat for all tokens in the read. This summation step simply requires a vector of incrementers, where each sum value is represented by $\lceil \log_2(\text{read_size}) \rceil$ bits. The maximum value that the final sum can be is equivalent to the size of the read simply due to the fact that that is the number of tokens that compose each read. The number of required sum values and incrementers is specified by p . After this has been repeated for all tokens in the read, we can reference the accumulators and compare the value to the required threshold to determine whether to discard a location.

In order to simplify referencing the accumulator, we utilize comparators for each of the accumulators after summing across each token. We can reduce the final accumulator values to a Boolean representing whether or not the read could possibly exist in the bin. Depending on the available bandwidth of the memory module in question, we simply require p incrementer lookup tables (LUT), p 7-bit counters (for our particular sets of 100 base pair reads), p comparators, and a single (num_bins)-bit vector that holds the final result for the given read at each bin. As future 3D-stacked memory devices are expected to have more parallelism, the hardware overhead increases linearly, but the performance overhead of GRIM-Filter reduces equally. GRIM-Filter requires a very small and simple logic layer which gives it an edge over other filtering algorithms that could be implemented on the logic layer.

5 Experimental Methodology

Evaluated Read Mapper. We evaluate our proposal using the state-of-the-art hash table based read mapper mrFAST with FastHASH [1]. We chose this mapper for our evaluations as it provides high accuracy in the presence of large error rates, which is required to detect genomic variants within and across species [1, 30]. However, we note that GRIM-Filter can be used with any other mapper.

Major Evaluation Metrics. We evaluate 1) the false negative rate (i.e., proportion of locations that pass the filter, but result in a poor match) of our GRIM-Filter, and 2) the performance improvement of the end-to-end read mapper when using GRIM-Filter. To obtain both results, we first integrate GRIM-Filter into mrFAST with FastHASH [1]. We measure the false negative rate of our filter (and the baseline filter used by the mapper) as the ratio of the number of locations that passed the filter but did not result in a mapping over all locations that passed the filter. We detail how we measure the performance improvement of our mechanism next.

Performance Evaluation. We measure the execution time improvement of our mechanism by taking three measurements: 1) execution time of the baseline mapper without GRIM-Filter (obtained by executing the source code of the mapper, which is available as open source [1]), 2) execution time of the baseline mapper with GRIM-Filter’s software implementation, which does not take advantage of emerging memory technologies (obtained by executing the source code of the baseline mapper integrated with our software version of GRIM-Filter, which we will make available

as open source software), 3) execution time of the baseline mapper with GRIM-Filter, which takes advantage of execution on 3D-stacked memory. To obtain the last entity, we measure the execution time of the software GRIM-Filter segments in mrFAST and subtract this from the obtained execution time in 2. Then, using a validated in-house simulator similar to Ramulator [31], we determine the overhead in offloading GRIM-Filter to a 3D-stacked memory system and add the overhead execution time to obtain the final execution time. We chose this methodology to estimate the runtime of GRIM-Filter on 3D-stacked memory technologies as such technologies that perform in-memory computation are unavailable to us at this point in time.

Evaluation System. Our evaluation system is an Intel(R) CoreTM i7-2600 CPU @ 3.40GHz with 16 GB of RAM for all experiments.

Data Sets. We used ten real data sets from the 1000 Genome Project Phase 1 1000 Genomes Project Consortium (2012). These were the same data sets used by Xin, et al [1] for a fair comparison. Table 1 lists the read length and size of each data set.

	ERR240726_1	ERR240727_1	ERR240728_1	ERR240729_1	ERR240730_1
No. of Reads	4031354	4082203	3894290	4013341	4082472
Read Length	100	100	100	100	100
	ERR240726_2	ERR240727_2	ERR240728_2	ERR240729_2	ERR240730_2
No. of Reads	4389429	4013341	4013341	4082472	4082472
Read Length	100	100	100	100	100

Table 1: Benchmark data, obtained from the 1000 Genomes Project Phase I [32]

6 Sensitivity Analysis and Results

We first profiled the reference human genome in order to determine a range of parameters that were reasonable to use for GRIM-Filter. We were able to determine the points of diminishing returns for several parameter values. This data is presented in Section 6.1. Using this preliminary data, we could reduce the required experiments to a reasonable range of parameters. Our implementation enabled the variation of runtime parameters (number of bins, token size, error threshold, etc.) within the ranges of values that we determined from our preliminary experimentation for the best possible results. We then were able to quantitatively evaluate the improvements in the false negative rate and runtime over mrFAST with FastHASH. Our results for the full mapper with GRIM-Filter are presented in Section 6.2.

6.1 Parameter Evaluation Results

In order to determine a range for the parameters that we used for experimentation, we ran a series of analyses on the fundamental characteristics of the human reference genome. Our initial experiments were designed to determine the *memory footprint* of our algorithm for effective performance improvements. To show how each of the different parameters affect the performance of GRIM-Filter, we study a preliminary sweep on the parameters with a range of values that would not incur excessive amounts of memory. Figure 6 shows how varying a number of different parameters affects the *average read existence* across the bins. We define average read existence to be the ratio of bins that pass the filter to all bins comprising the genome, for a representative set of reads. We want this value to be as low as possible because it reflects the filter’s ability to filter incorrect mappings. The fewer bins that these reads, in the representative set, map result in possible mappings, the more likely it

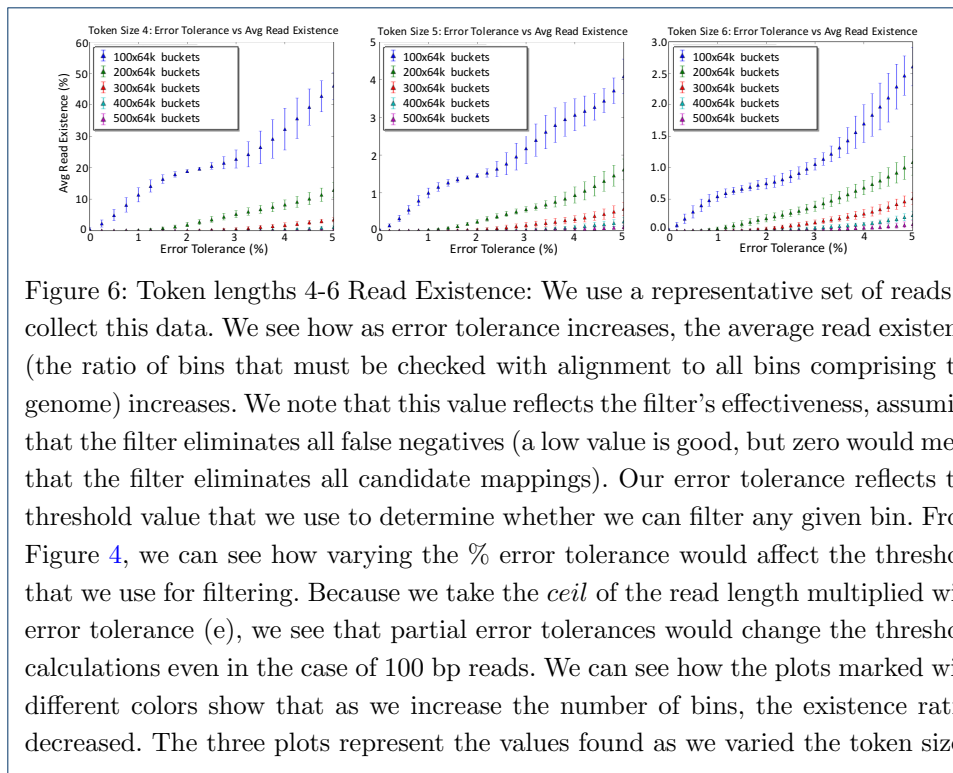


Figure 6: Token lengths 4-6 Read Existence: We use a representative set of reads to collect this data. We see how as error tolerance increases, the average read existence (the ratio of bins that must be checked with alignment to all bins comprising the genome) increases. We note that this value reflects the filter’s effectiveness, assuming that the filter eliminates all false negatives (a low value is good, but zero would mean that the filter eliminates all candidate mappings). Our error tolerance reflects the threshold value that we use to determine whether we can filter any given bin. From Figure 4, we can see how varying the % error tolerance would affect the threshold that we use for filtering. Because we take the *ceil* of the read length multiplied with error tolerance (e), we see that partial error tolerances would change the threshold calculations even in the case of 100 bp reads. We can see how the plots marked with different colors show that as we increase the number of bins, the existence ratios decreased. The three plots represent the values found as we varied the token size.

will be that we will not have to align a given location. Across the three plots, we vary the token size from 4 to 6. Within each plot, we vary the number of bins to split the reference genome into, denoted by the different colors. The x-axis varies the error threshold between a match, and the y-axis shows average read existence. We plot the average and min/max across our 10 data sets (Table 1) as indicated respectively by the triangle and whiskers. We make *three* observations. First, we observe, across the three plots, that increasing the *token size*, from 4 to 5, shows massive drops in the read existence while 5 to 6 exhibits significantly diminishing returns. This is due to the fact that, given a random pool of A,C,T,G’s, the probability of observing a substring of size q is $(\frac{1}{4})^q$. However, due to the non-uniform distribution of base pairs across the genome and the bin sizes, we see diminishing returns on the average read existence. Second, we observe that across the plots, each increase in the number of bins results in a decrease in the read existence. This is understandable due to the fact that the bin size decreases as the number of bins increases and for smaller bins, we have a smaller sample size that any given substring could exist within. When sweeping the number of bins, we use multiples of 64k because it is an even multiple of the number of TSVs between the logic and memory layers in today’s 3D-stacked memories. We want to use a multiple of 64k so that we can utilize all TSVs for each access. Third, we observe that for each plot, increasing the error threshold results in an increase in the read existence. This is due to the fact that if we allow errors, a wider variety of sequences map to the same read. We conclude from this figure that using tokens of size 5 gives the best tradeoff between memory consumption and filtering efficiency.

To show how we chose our final bit vector size to use for experimentation, we sweep the number of bins and the error threshold ($e\%$). Figure 7 shows how varying these parameters affects the false negative rates of the filtering algorithm. The x-

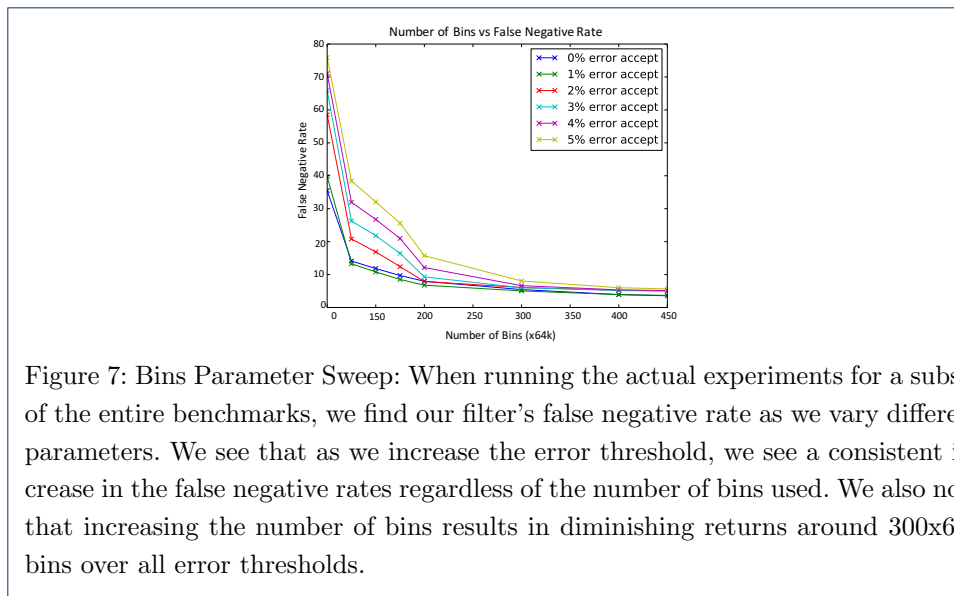


Figure 7: Bins Parameter Sweep: When running the actual experiments for a subset of the entire benchmarks, we find our filter’s false negative rate as we vary different parameters. We see that as we increase the error threshold, we see a consistent increase in the false negative rates regardless of the number of bins used. We also note that increasing the number of bins results in diminishing returns around 300x64k bins over all error thresholds.

axis varies the number of bins, while the different colors represent the different error thresholds. We make two observations from this plot. First, we find that with more bins (thus a smaller bin size), the false negative rate (i.e., the number of locations that pass through the filter, but don’t result in a mapping after alignment) decays exponentially. After 300x64k bins, we start to see diminishing returns on the reduction of false negatives for all error thresholds. Second, we observe that as we increase the error threshold, we see that regardless of the other parameters, the false negative rates increase. However, we can take advantage of the convergence of the different error thresholds depending on the number of bins. After approximately 300x64k bins, we see very small differences in the false negative rates for differing error thresholds. Due to the slight improvements for false negative rates with an increasing number of bins and the fact that number of bins minimally affects the runtime of our filtering algorithm, we choose a value that reflects a reasonable memory footprint given the other parameters. We conclude that employing 450x64k bins results in the best tradeoff between memory consumption, filtering efficiency, and runtime. We note that the time to generate the bit vectors is not included in our final runtime results because they only need to be generated once per genome, either by the user or by the distributor. However, for a better sense of the timescale, we find that with a genome length L , we can generate the bit vectors in $9.03e-08 * L$ seconds when using $450 * 64k$ bins (this is approximately 5 minutes for the human genome).

Because the increasing number of bins results in more bit vectors, we must keep this parameter at a reasonable value in order to retain a reasonable memory footprint. Since we have chosen a token size of 5, we will require t bit vectors with a length of $4^5 = 1024$, where t equals the number of bins we segment the reference genome into. We choose 450x64k bins as a reasonable tradeoff between memory footprint and false negative rate. This set of parameters result in a total memory footprint of approximately 3.8 GB for storing the bit vectors of this mechanism, which is a reasonable size for today’s 3D-stacked memories.

We ran several experiments to examine the benefits behind GRIM-Filter’s ability to parallelize consecutive bins. We noticed significant benefit in exploiting paral-

lelism when p is 4096 (which is the bandwidth for HBM2) [10]. In approximately 10% of the k -mers, we see a significant decrease (98.6%) in required window retrievals. In the remaining k -mers, we see approximately 10-20% decrease in required window retrievals. From HBM2 specifications [10], we note that the available bandwidth between memory and logic layer is 4096 bits, therefore our chosen experimental p value was 4096. Given larger p values, we have experimental data showing a continual reduction of required window retrievals.

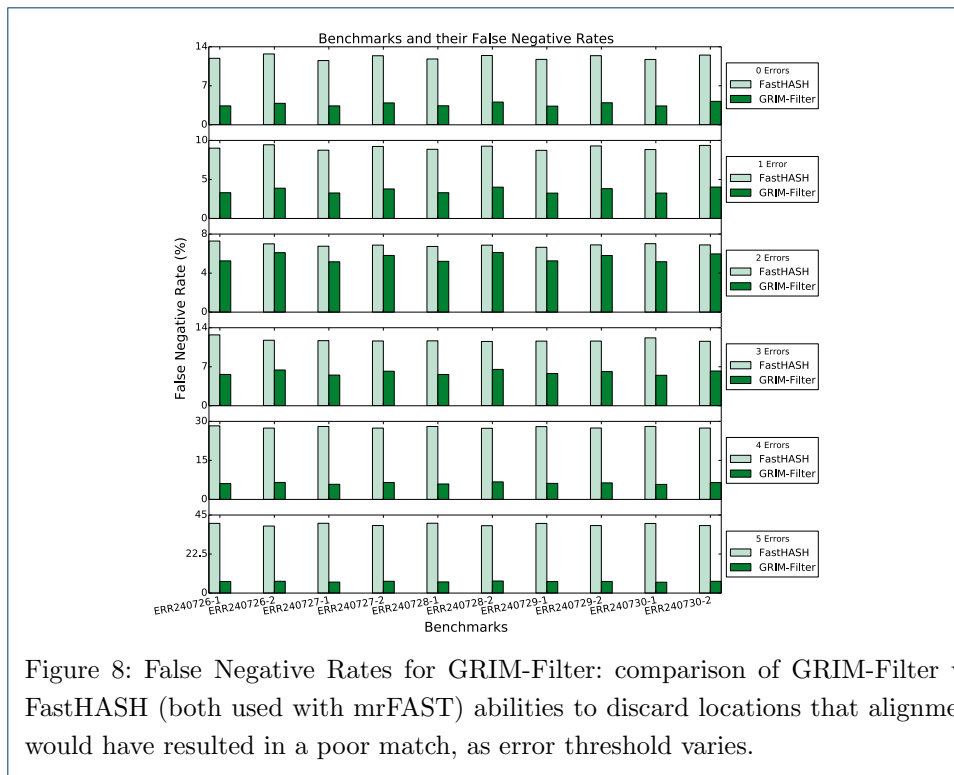
6.2 Full Mapping Results

We used a popular seed-and-extend mapper, mrFAST [30], to retrieve all candidate mappings from ten real data sets from the 1000 Genome Project Phase I [32]. Table 1 lists the number of reads and size of each read in each benchmark. In our experiments we use a token of length 5 and 450x64k bins as discussed in Section 6.1.

Figure 8 shows the number of false negative locations that pass through GRIM-Filter compared to the baseline. The shared x-axis indicates the ten sets of reads and the y-axis indicates the false negative rate. The light green and dark green respectively mark the baseline and GRIM-Filter, and the graphs descending vary in error thresholds. We make two observations. First, we note a significantly lower false negative rate for all benchmarks in all ranges of error thresholds when compared to the results of FastHASH. Second, we observe a phenomenon where the false negative rates increase when increasing the error threshold from 0% to 2% and then decrease from 3% to 5%. We attribute this to a combination of factors. This includes the fact that increasing the error threshold results in more acceptable mapping locations. However, the number of candidate locations do not change. This naturally results in a smaller false negative rate. There is another underlying factor: as acceptable error threshold increases, our thresholding value decreases and allows for more locations to pass through the filter resulting in an increased false negative rate. We conclude that the interaction of these two factors are the cause for the initial increase and later decrease in the false negative rates. We note that when using this filter for higher error threshold, we observe larger improvements in the false negative rate which can be reflected in the runtime. When comparing our filtering algorithm to FastHASH for an error threshold of 5%^[1], we see that our algorithm results in *5.97x* less false negative locations on average across the benchmarks. This is reflected directly as a decrease in the end-to-end runtime, since fewer locations must be fully aligned.

Figure 9 compares the execution time of GRIM-Filter against the baseline, mrFAST with FastHASH. This graph follows the same format as the previous, except the y-axis now represents the execution time scaled to 1000 seconds. We make two observations. First, we observe that GRIM-Filter shows performance improvement over all benchmarks regardless of the error threshold. Second, as the error threshold increases, we gain increasingly more performance benefit. This is due to the fact that GRIM-Filter is able to discard many more locations than FastHASH at higher error thresholds, thus saving much more execution time by ignoring unnecessary alignments. Again, because of the importance of high sensitivity for calling structural variations and the direct correlation between runtime and error threshold, we report all numbers only looking at the maximum error threshold of 5%. When we compare the runtime of mrFAST with GRIM-Filter against the previous fastest read mapper, mrFAST with FastHASH, we find a 2.08x (3.65x) performance boost on average (max) across the benchmarks. When we further break down the computation time, we find that our performance gains are from an average decrease

^[1]It is most important to compare to 5% error threshold as it is the accepted worst case error rate for read mappers and provides the highest sensitivity.



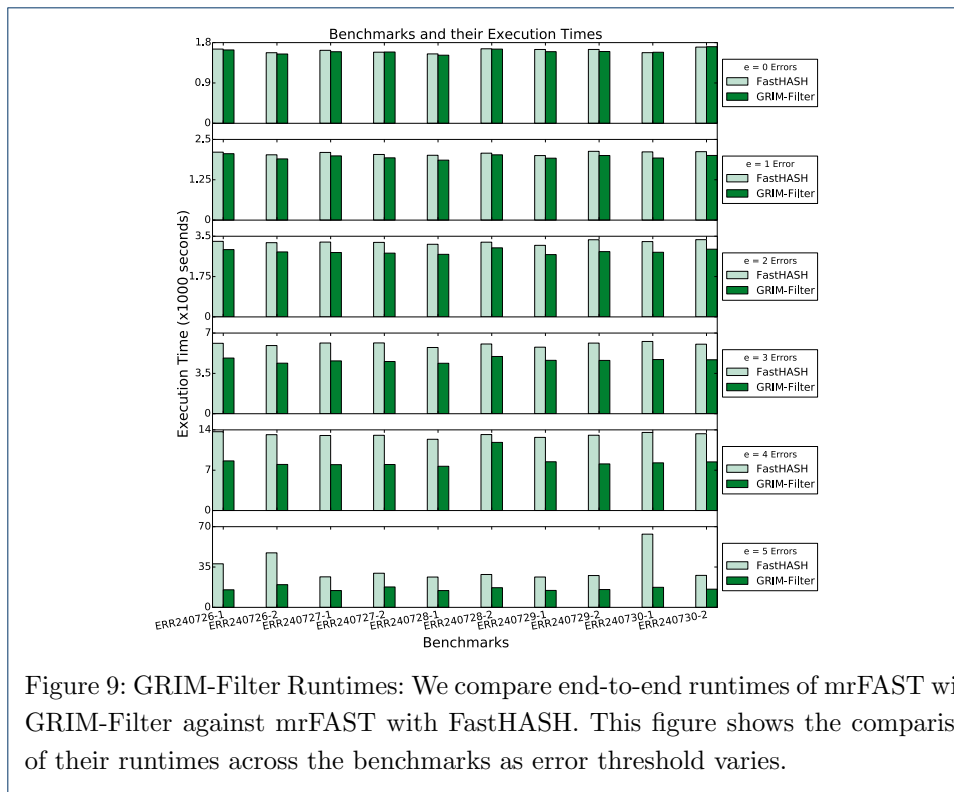
across datasets of 83.7% computation time on false negative locations. We conclude that employing GRIM-Filter can significantly enhance the performance of a state-of-the-art mapper.

7 Related Works

To our knowledge, this is the first paper to exploit 3D-stacked DRAM and its processing-in-memory capabilities to overcome the recent bottleneck shift to memory bandwidth in read mapping due to the immense improvement on the prior bottleneck, alignment. In this section, we briefly describe related works that aim to accelerate read mapping with hardware support.

Many prior works used FPGAs to accelerate alignment. These include [33–43] and all accelerate read mapping using customized FPGA implementations of different existing read mapping algorithms. Arram et al. [35] accelerate SOAP3 tool on an FPGA engine and it shows up to $134x$ speedup compared to BWA. Houtgast et al. [39] present a FPGA-accelerated version of BWA-MEM that is $3x$ faster compared to its software implementation. Other works use GPUs [44–47] for the same purpose. Liu et al. [45] accelerate BWA and Bowtie by $7.5x$ and $20x$, respectively. However, all these accelerators are still bottlenecked by memory bandwidth. Compared to these accelerators, our approach overcomes the memory bandwidth bottleneck by utilizing the up-and-coming 3D-stacked DRAM with a newly designed algorithm that is specific to this technology.

In the case of other hardware optimized implementations with much higher speedups, they focus on the acceleration of the actual alignment (the dynamic programming step) which is the bulk of the computation in mapping. While many works have managed to attain the maximum possible acceleration in alignment through multiple iterations of implementations ranging from ASIC to FPGA, we



explore a newer area in mapping that requires significantly less computation. We show that we can accelerate the entire mapping pipeline by utilizing the inherent massive parallelism in 3D-DRAM. We note that GRIM-Filter is orthogonal to other filters and mapper steps and can be stacked on top of other existing optimizations for further potential acceleration. We show that when we run mapping with GRIM-Filter on a commodity CPU, we see $1.81x - 3.65x$ performance improvement. We speculate substantial potential in tying together the implementation of this filter with other hardware optimized aligners.

8 Conclusion

We introduced a new algorithm, GRIM-Filter, for accelerating genome read mapping. GRIM-Filter takes advantage of an emerging technology, 3D-stacked memory, which enables the efficient use of processing-in-memory to overcome the memory bottleneck in read mapping today. We utilize the processing-in-memory capability of 3D-stacked technology and exploit its massive internal bandwidth to run GRIM-Filter which efficiently and quickly filters large segments of the genome for later steps of read mapping. With the most relevant alignment error acceptance rate of 5%, we show that GRIM-Filter filters locations with approximately $5.59x-6.41x$ smaller false negative rate than FastHASH and performs $1.81x-3.65x$ faster than the fastest read mapper, mrFAST with FastHASH. GRIM-Filter is a universal filter that can be applied to any read mapper.

We believe there is huge potential in adapting DNA read mapping algorithms to state-of-the-art and emerging memory and processing technologies. With our results, we hope that our paper, which introduces the first work in doing so for 3D-stacked memories, which are increasingly common in today's computing landscape,

provides inspiration for other such works to design new sequence analysis algorithms that take advantage of 3D-stacked memory.

Author details

¹Department of Electrical and Computer Engineering, Carnegie Mellon University, Forbes Avenue, Pittsburgh, USA. ²Department of Computer Science, Carnegie Mellon University, Forbes Avenue, Pittsburgh, USA. ³NVIDIA Research, Austin, USA. ⁴Department of Computer Engineering, Bilkent University, Bilkent, Ankara, Turkey, Bilkent, TR. ⁵ Department of Computer Engineering, TOBB University of Economics and Technology, Sogutozu, TR. ⁶ Department of Computer Science, Systems Group, Zurich, CH.

References

- Xin, H., Lee, D., Hormozdiari, F., Yedkar, S., Mutlu, O., Alkan, C.: Accelerating read mapping with FastHASH. *BMC genomics* **14**(Suppl 1), 13 (2013)
- Xin, H., Greth, J., Emmons, J., Pekhimenko, G., Kingsford, C., Alkan, C., Mutlu, O.: Shifted Hamming distance: a fast and accurate SIMD-friendly filter to accelerate alignment verification in read mapping. *Bioinformatics*, 856 (2015)
- Tran, N.H., Chen, X.: AMAS: optimizing the partition and filtration of adaptive seeds to speed up read mapping. arXiv preprint arXiv:1502.05041 (2015)
- Xin, H., Nahar, S., Zhu, R., Emmons, J., Pekhimenko, G., Kingsford, C., Alkan, C., Mutlu, O.: Optimal Seed Solver: Optimizing Seed Selection in Read Mapping. *Bioinformatics*, 670 (2015)
- Alser, M., Hassan, H., Xin, H., Ergin, O., Mutlu, O., Alkan, C.: GateKeeper: A New Hardware Architecture for Accelerating Pre-Alignment in DNA Short Read Mapping. *Bioinformatics* (2017). doi:10.1093/bioinformatics/btx342
- Alser, M., Mutlu, O., Alkan, C.: Magnet: Understanding and improving the accuracy of genome pre-alignment filtering. *The IPSI BgD Transactions on Internet Research* (2017)
- High Bandwidth Memory — Reinventing Memory Technology. <http://www.amd.com/en-us/innovations/software-technologies/hbm>. Accessed: 2016-01-26
- Lee, D., Ghose, S., Pekhimenko, G., Khan, S., Mutlu, O.: Simultaneous multi-layer access: Improving 3D-stacked memory bandwidth at low cost. *Architecture and Code Optimization, ACM Transactions on* (2016)
- AMD Radeon TM R9 Series Graphics Cards with High-Bandwidth Memory. <http://www.amd.com/en-us/products/graphics/desktop/r9>. Accessed: 2016-01-26
- O'Connor, M.: Highlights of the High-Bandwidth Memory (HBM) Standard. In: *Memory Forum Workshop* (2014)
- Hybrid Memory Cube Controller IP Core User Guide. Accessed: 2016-01-26
- Hybrid Memory Cube Member Tool Resources. <http://hybridmemorycube.org/tool-resources.html>. Accessed: 2016-01-26
- Ahmadi, A., Behm, A., Honnalli, N., Li, C., Weng, L., Xie, X.: Hobbes: optimized gram-based methods for efficient read alignment. *Nucleic Acids Research* **40**(6), 41–41 (2012)
- Cheng, H., Jiang, H., Yang, J., Xu, Y., Shang, Y.: Bitmapper: an efficient all-mapper based on bit-vector computing. *BMC bioinformatics* **16**(1), 192 (2015)
- Hatem, A., Bozdağ, D., Toland, A.E., Çatalyürek, Ü.V.: Benchmarking short sequence mapping tools. *BMC bioinformatics* **14**(1), 184 (2013)
- Mutlu, O., Stark, J., Wilkerson, C., Patt, Y.N.: Runahead execution: An effective alternative to large instruction windows. *IEEE Micro* (6), 20–25 (2003)
- Kim, D.H., Athikulwongse, K., Lim, S.K.: A study of through-silicon-via impact on the 3D stacked IC layout. In: *Proceedings of the 2009 International Conference on Computer-Aided Design*, pp. 674–680 (2009). ACM
- Dlugosch, P., Brown, D., Glendenning, P., Leventhal, M., Noyes, H.: An efficient and scalable semiconductor architecture for parallel automata processing. *Parallel and Distributed Systems, IEEE Transactions on* **25**(12), 3088–3098 (2014)
- In-Memory Computing. <http://www.tibco.com/products/automation/in-memory-computing>. Accessed: 2016-01-26
- Micron Automata Processing. <http://www.micronautomata.com/hardware>. Accessed: 2016-01-26
- Ahn, J., Hong, S., Yoo, S., Mutlu, O., Choi, K.: A scalable processing-in-memory accelerator for parallel graph processing. In: *Proceedings of the 42nd Annual International Symposium on Computer Architecture*, pp. 105–117 (2015). ACM
- Ahn, J., Yoo, S., Mutlu, O., Choi, K.: PIM-enabled instructions: a low-overhead, locality-aware processing-in-memory architecture. In: *Proceedings of the 42nd Annual International Symposium on Computer Architecture*, pp. 336–348 (2015). ACM
- Seshadri, V., Hsieh, K., Boroumand, A., Lee, D., Kozuch, M., Mutlu, O., Gibbons, P., Mowry, T.: Fast Bulk Bitwise AND and OR in DRAM (2015)
- Seshadri, V., Kim, Y., Fallin, C., Lee, D., Ausavarungnirun, R., Pekhimenko, G., Luo, Y., Mutlu, O., Gibbons, P.B., Kozuch, M.A., et al.: Rowclone: Fast and energy-efficient in-DRAM bulk data copy and initialization. In: *Proceedings of the 46th Annual IEEE/ACM International Symposium on Microarchitecture*, pp. 185–197 (2013). ACM
- Seshadri, V., Mullins, T., Boroumand, A., Mutlu, O., Gibbons, P.B., Kozuch, M.A., Mowry, T.C.: Gather-scatter DRAM: In-DRAM address translation to improve the spatial locality of non-unit strided accesses. In: *Proceedings of the 48th International Symposium on Microarchitecture*, pp. 267–280 (2015). ACM
- Akin, B., Franchetti, F., Hoe, J.C.: Data reorganization in memory using 3D-stacked DRAM. In: *Computer Architecture (ISCA), 2015 ACM/IEEE 42nd Annual International Symposium On*, pp. 131–143 (2015). IEEE
- Guo, Q., Alachiotis, N., Akin, B., Sadi, F., Xu, G., Low, T.M., Pileggi, L., Hoe, J.C., Franchetti, F.: 3D-stacked memory-side acceleration: Accelerator and system design. In: *In the Workshop on Near-Data Processing (WoNDP)(Held in Conjunction with MICRO-47.)* (2014)
- Loh, G.H.: 3D-stacked memory architectures for multi-core processors. In: *ACM SIGARCH Computer Architecture News*, vol. 36, pp. 453–464 (2008). IEEE Computer Society
- Zhu, Q., Akin, B., Sumbul, H.E., Sadi, F., Hoe, J.C., Pileggi, L., Franchetti, F.: A 3D-stacked logic-in-memory accelerator for application-specific data intensive computing. In: *3D Systems Integration Conference (3DIC), 2013 IEEE International*, pp. 1–7 (2013). IEEE

30. Alkan, C., Kidd, J.M., Marques-Bonet, T., Aksay, G., Antonacci, F., Hormozdiari, F., Kitzman, J.O., Baker, C., Malig, M., Mutlu, O., *et al.*: Personalized copy number and segmental duplication maps using next-generation sequencing. *Nature genetics* **41**(10), 1061–1067 (2009)
31. Kim, Y., Yang, W., Mutlu, O.: Ramulator: A fast and extensible dram simulator (2015)
32. 1000 Genomes Project Consortium: An integrated map of genetic variation from 1,092 human genomes. *Nature* **491**(7422), 56–65 (2012). doi:[10.1038/nature11632](https://doi.org/10.1038/nature11632)
33. Aluru, S., Jammula, N.: A review of hardware acceleration for computational genomics. *Design & Test, IEEE* **31**(1), 19–30 (2014)
34. Arram, J., Tsoi, K.H., Luk, W., Jiang, P.: Hardware acceleration of genetic sequence alignment. In: *Reconfigurable Computing: Architectures, Tools and Applications*, pp. 13–24. Springer, ??? (2013)
35. Arram, J., Tsoi, K.H., Luk, W., Jiang, P.: Reconfigurable acceleration of short read mapping. In: *Field-Programmable Custom Computing Machines (FCCM), 2013 IEEE 21st Annual International Symposium On*, pp. 210–217 (2013). IEEE
36. Ashley, E.A., Butte, A.J., Wheeler, M.T., Chen, R., Klein, T.E., Dewey, F.E., Dudley, J.T., Ormond, K.E., Pavlovic, A., Morgan, A.A., *et al.*: Clinical assessment incorporating a personal genome. *The Lancet* **375**(9725), 1525–1535 (2010)
37. Chiang, J., Studniberg, M., Shaw, J., Seto, S., Truong, K.: Hardware accelerator for genomic sequence alignment. In: *Engineering in Medicine and Biology Society, 2006. EMBS'06. 28th Annual International Conference of the IEEE*, pp. 5787–5789 (2006). IEEE
38. Hasan, L., Al-Ars, Z., Vassiliadis, S.: Hardware acceleration of sequence alignment algorithms-an overview. In: *Design & Technology of Integrated Systems in Nanoscale Era, 2007. DTIS. International Conference On*, pp. 92–97 (2007). IEEE
39. Houtgast, E.J., Sima, V.-M., Bertels, K., Al-Ars, Z.: An FPGA-based systolic array to accelerate the BWA-MEM genomic mapping algorithm. In: *Embedded Computer Systems: Architectures, Modeling, and Simulation (SAMOS), 2015 International Conference On*, pp. 221–227 (2015). IEEE
40. McMahon, P.L.: *Accelerating Genomic Sequence Alignment using High Performance Reconfigurable Computers*. PhD thesis, University of California, Berkeley (2008)
41. Olson, C.B., Kim, M., Clauson, C., Kogon, B., Ebeling, C., Hauck, S., Ruzzo, W.L.: Hardware acceleration of short read mapping. In: *Field-Programmable Custom Computing Machines (FCCM), 2012 IEEE 20th Annual International Symposium On*, pp. 161–168 (2012). IEEE
42. Papadopoulos, A., Kirmizoglou, I., Promponas, V.J., Theocharides, T.: FPGA-based hardware acceleration for local complexity analysis of massive genomic data. *Integration, the VLSI Journal* **46**(3), 230–239 (2013)
43. Waidyasooriya, H.M., Hariyama, M., Kameyama, M.: FPGA-Accelerator for DNA Sequence Alignment Based on an Efficient Data-Dependent Memory Access Scheme. *Highly-Efficient Accelerators and Reconfigurable Technologies*, 127–130 (2014)
44. Blom, J., Jakobi, T., Doppmeier, D., Jaenicke, S., Kalinowski, J., Stoye, J., Goesmann, A.: Exact and complete short-read alignment to microbial genomes using Graphics Processing Unit programming. *Bioinformatics* **27**(10), 1351–1358 (2011)
45. Liu, C.-M., Wong, T., Wu, E., Luo, R., Yiu, S.-M., Li, Y., Wang, B., Yu, C., Chu, X., Zhao, K., *et al.*: SOAP3: ultra-fast GPU-based parallel alignment tool for short reads. *Bioinformatics* **28**(6), 878–879 (2012)
46. Luo, R., Wong, T., Zhu, J., Liu, C.-M., Zhu, X., Wu, E., Lee, L.-K., Lin, H., Zhu, W., Cheung, D.W., *et al.*: SOAP3-dp: fast, accurate and sensitive GPU-based short read aligner (2013)
47. Manavski, S.A., Valle, G.: CUDA compatible GPU cards as efficient hardware accelerators for Smith-Waterman sequence alignment. *BMC bioinformatics* **9**(Suppl 2), 10 (2008)